Environ Sci Pollut Res (2017) 24:782–794
DOI 10.1007/s11356-016-7795-6

RESEARCH ARTICLE

Phenolic resin-derived activated carbon-supported divalent metal as efficient adsorbents (M–C, M=Zn, Ni, or Cu) for dibenzothiophene removal

Chi He[1] · Gaoshan Men[1] · Bitao Xu[1] · Jin Cui[1] · Jinglian Zhao[1]

Received: 28 March 2016 / Accepted: 28 September 2016 / Published online: 18 October 2016

Abstract The adsorption process and mechanism of dibenzothiophene (DBT) over metal-loaded phenolic resin-derived activated carbon (PR-AC) were firstly reported in this work. The metal component (Zn, Ni, or Cu) was respectively introduced to PR-AC support via an impregnation method. The effects of adsorbent component, initial DBT concentration, liquid hourly space velocity (LHSV), adsorption time, and adsorption temperature on the adsorption capacity of the adsorbents were systematically investigated. Furthermore, the adsorption mechanism was discussed by analyzing the properties of adsorption product and saturated adsorbent as well as adsorption kinetics. Experimental results indicate that the PR-AC-loaded metal adsorbents, especially with Zn, present much higher DBT adsorption capability than that of pure PR-AC support. The DBT removal rate over PR-AC-loaded Zn (Zn^{2+} = 0.2 mol L^{-1}) reaches 89.14 %, which is almost twice higher than that of pure PR-AC (45.6 %). This is due to the π-complexation between DBT and metal ions (dominating factor) and the weakening of the local hard acid sites over PR-AC. The multi-factor orthogonal experiment shows that the DBT removal rate over PR-AC-loaded Zn sample achieved 92.36 % in optimum conditions.

Responsible Editor: Philippe Garrigues

Electronic supplementary material The online version of this article (doi:10.1007/s11356-016-7795-6) contains supplementary material, which is available to authorized users.

✉ Chi He
chi_he@xjtu.edu.cn

[1] Department of Environmental Science and Engineering, School of Energy and Power Engineering, Xi'an Jiaotong University, Xi'an 710049, People's Republic of China

Keywords Dibenzothiophene · Adsorption · Activated carbon · Metal sites · Phenolic resin

Introduction

Deep desulfurization of diesel fuel has recently attracted more and more attentions due to the release of sulfur oxides (SO_x) during combustion of sulfur-containing diesel oil. SO_x is a kind of main pollutants in the atmosphere, which can form acid rain and hence destroy ecological environment. Additionally, SO_x can also increase the emissions of CH, CO, nitrogen oxides (NO_x), and particulate pollutants in exhaust, corrode engine parts of automobile, and poison the catalytic converter (Song and Ma 2003). To minimize the air pollution caused by SO_x, regulations that limit the sulfur levels of diesel are becoming increasingly stringent in lots of countries (Stanislaus et al. 2010). For example, in 2004, the US Environmental Protection Agency (EPA) signed the final rule introducing Tier 4 emission standards which stipulated that ultra-low sulfur diesel (15 ppm) was effective in June 2010 for nonroad fuel and June 2012 for locomotive and marine fuels. Therefore, it is imperative to produce lower sulfur diesel oil to meet the demand of severe regulations. However, the sulfur content in gasoline or diesel fuel cannot be reduced to less than 20 ppm by common technology of desulfurization or hydrodesulphurization (HDS) (Seredych et al. 2009) which needs severe operating conditions (e.g., high temperature and high pressure) and large hydrogen consumption (Bhatia and Sharma 2012). Especially, these technologies cannot remove benzothiophenes (BTs) and dibenzothiophenes (DBTs) in fuels efficiently (Dharaskar et al. 2015). As a consequence, other alternative ways such as oxidative desulfurization (ODS), extraction, biodesulfurization (BDS), and adsorptive desulfurization (ADS) have been developed. ODS methods

are usually followed by extraction or adsorption through which the oxidized sulfur compounds can be separated from the oil (Yu and Wang 2013). However, the ODS approaches still cannot be used to industrial applications because of some difficulties in the reactivation of deactivated catalyst and the treatment of oxidized sulfur compounds although DBTs in oils can be efficiently removed (Kulkarni and Afonso 2010). As an environment-friendly and low-cost method, BDS has drawn wide attentions recently, while the development of BDS is limited due to the slowness of removal process (Srivastava 2012). ADS which uses adsorbents to remove sulfur compounds in fuels via selective adsorption is a new technology developed in recent years. ADS has the capability to reduce sulfur content in oils to lower than 1.0 ppm under mild conditions and can make the color of products purer without using costly hydrogen compared with the HDS (Xiao et al. 2013). Numerous studies have focused on ADS for its low cost, high desulfurization efficiency, low octane number loss, and good market prospect (Wang et al. 2009; Fallah et al. 2014).

The key issue of ADS technology is to develop efficient adsorbents that are highly selective to adsorb thiophenic compounds and have medium affinities to aromatics, but not adsorb alkanes and branched alkanes (Hernández-Maldonado and Yang 2004a). There are various adsorbents that can remove sulfur compounds in fuels such as activated carbon, zeolites, and metal oxides such as activated alumina. Yang and coworkers have developed π-coordination adsorption for thiophenic compounds (TC) using zeolite-supported adsorbents (i.e., Ag-Y, Cu(I)-Y, Ni(II)-Y, and Ni(II)-X) (Hernández-Maldonado and Yang 2003, 2004b, c, d; Yang et al. 2003). Black & Veath Pritchard Industry and Alcoa Industrial Chemicals have developed a low-cost process named Irvad using activated alumina as the sorbent. It is claimed that the sulfur content in the products treated by Irvad is only 0.5 ppm (Irvine 1998). Another commercialized technology is S-Zorb diesel process proposed by Conoco Phillips, in which ZnO is the main component of the adsorbent, and less hydrogen is consumed than in HDS process (Khare et al. 2000; Zhang et al. 2012). Additionally, other adsorbents were also studied including nickel or nickel oxide-impregnated orbent support comprising zinc oxide, expanded perlite, and alumina (Seredych and Bandosz 2010; Reed et al. 2003), rice husk ash modified with niobium (Cavalcantia et al. 2015), and microporous coordination polymers (Cychosz et al. 2009). However, most of these adsorbents are very difficult to be widely used in practical applications.

Activated carbon is a kind of commercially available adsorbent, while common activated carbon with relatively low specific surface area (around 800 $m^2\ g^{-1}$) and great amounts of impurities or ash cannot meet the demand of growing industry (Tennison 1998). Much attentions have been paid to phenolic resin-derived activated carbon due to its rapid adsorption, concentrated pores, high hardness, and promoted and controllable specific surface area (1000–3000 $m^2\ g^{-1}$), pore radius (9–22 A), and pore volume (0.22–1.2 mL g^{-1}) (Nakagawa et al. 2007; Singh and Lal 2008; Lei et al. 2013). To further enhance the adsorption properties of activated carbon, numerous researchers explored modification of activated carbon such as oxidation or metal impregnation. It is reported that DBT adsorption can be particularly enhanced by transitional metal ion-loaded activated carbon. Seredych et al. have investigated the adsorption of DBT and dimethyldibenzothiophene (DMDBT) on polymer-derived carbons with copper and iron active phases and found that the volume of micropores governed the adsorption capacity (Seredych and Bandosz 2010). Thaligari et al. (2016) used zinc-impregnated granular activated carbon as adsorbent for the removal of DBT from iso-octane and found that higher temperature enhanced the desulfurization process. Moosavi et al. (2012) assessed the impact of different metal species on the adsorption of thiophenic compounds over metal-loaded activated carbon fiber and reported that Cu_2O or NiO species showed the highest uptakes. It was also reported that the application of ultrasound irradiation to prepare metal ion-impregnated activated carbon can improve the adsorption capacities of DBT (Xiao et al. 2010).

To develop a kind of more efficient and applicable adsorbent for desulfuration, a series of desulfurization adsorbents were synthesized with high-performance phenolic resin-derived activated carbon (PR-AC) and different amounts of Cu^{2+}, Zn^{2+}, or Ni^{2+} divalent cations for DBT adsorption in model diesel fuel in this work. A remarkable desulfurization rate (92.36 %), which was much higher than that of other commercial adsorbents reported in the literature (Dharaskar et al. 2015; Cavalcanti et al. 2013; Zhao et al. 2008; Moosavi et al. 2012; Muzic et al. 2010), was obtained under optimum conditions. The effects of adsorbent component, initial DBT concentration, liquid hourly space velocity, adsorption time, and adsorption temperature on the adsorption capacity of adsorbents were systematically investigated for adsorption desulfurization; 2123-phenolic resin was used to prepare the PR-AC support by steam activation method. The desulfurization mechanism was also elucidated and revealed that the principle of DBT adsorption is selective adsorption governed by the coordinated action of π mainly.

Experimental

Adsorbent preparation

Synthesis of phenolic resin-derived activated carbon

The CAS number and purity of all chemicals are listed in Table S1. The Novolac-type phenolic resin and hexamethylenetetramine were respectively used as the carbon precursor

and curing agent (Yang et al. 2002), and they were dissolved in methanol in different proportions (100:6, 100:9, 100:12, *w*/*w*). After thorough mixing, the methanol in the mixture was evaporated off under reduced pressure to obtain solid particles. After that, 200 mL of diethylamine tetraacetic acid disodium aqueous solution was placed in a high-pressure reactor followed by adding the particles and heated to 125 °C for 2 h at a rate of about 2 °C min^{-1} under vigorous stirring. Globular phenolic resin particles were obtained after the high-pressure reactor was cooled to room temperature. Finally, PR-AC was prepared by carbonizing the globular phenolic resin particles via a two-stage heating at 250 and 800 °C for 1 h under nitrogen atmosphere, and activating at 750 °C under a steam stream (Zhao et al. 2009). The PR-AC with the novolac-type phenolic resin to hexamethylenetetramine ratio of 100:9 (*w*/*w*) was denoted as C-PR.

Synthesis of desulfurization adsorbent

Firstly, the C-PR was washed repeatedly with distilled water to remove the inorganic impurities from the surface, and the obtained material was further washed with nitric acid (0.1 mol L^{-1}) and distilled water. Next, the organic impurities over C-PR were removed by using the sodium hydroxide aqueous solution (0.1 mol L^{-1}), and then washed with distilled water until the filtrate was neutral. After drying at 100 °C for 12 h, 10 g of the preprocessed C-PR was impregnated respectively in 100 mL of $Zn(NO_3)_2$, $Ni(NO_3)_2$, and $Cu(NO_3)_2$ solutions (Dhawan et al. 2015) with various concentrations (0.05, 0.1, 0.2, 0.3, 0.4, and 0.5 mol L^{-1}) for 12 h at room temperature (Xiao et al. 2010). Finally, the products were dried at 100 °C for 24 h and calcined at 750 °C for 2 h under nitrogen atmosphere to obtain the desulfurization adsorbents with different metal loading contents, denoted as Zn–C–*X*, Ni–C–*X*, and Cu–C–*X* (*X* = 0.05, 0.1, 0.2, 0.3, 0.4, and 0.5), respectively.

Adsorbent characterizations

Transmission electron microscopy (TEM) images of C-PR and Zn–C samples were obtained using a JEOL JEM-200CX microscope operating at an acceleration voltage of 200 kV. Scanning electron microscopy (SEM) images were obtained using a JEOL JSM-6700F microscope equipped with an EDX detector. N_2 adsorption/desorption isotherms of the catalysts were measured at 77 K using a F-sorb 3400 gas sorption analyzer. Before the measurement, all samples were degassed under vacuum at 130 °C for 3 h before measurement. The total pore volume was estimated from the amount of nitrogen adsorbed at a relative pressure (P/P_0) of ca. 0.99. The specific surface area was calculated using the Brunauer–Emmett–Teller (BET) method, and the pore size distribution was derived from the adsorption branch of the N_2 isotherm using the Barrett–Joyner–Halenda (BJH) method. The compositions of the desulfurization adsorbents were detected by a Bruker Tensor37 Fourier translation infrared spectroscopy (FT-IR), all spectra were collected at a resolution of 4 cm^{-1} with 100 scans.

Model diesel fuel preparation

The initial model diesel fuel was prepared by adding different volume (10, 20, 30, 40, 50, 60, 70, and 80 mL) of DBT stock solution (1000 mg L^{-1}) into volumetric flasks (100 mL). Then *n*-octane was put in the volumetric flasks resulting in 100 mL of DBT solution with different concentrations (100, 200, 300, 400, 500, 600, 700, and 800 mg L^{-1}).

Desulfuration performance

Adsorption experiment

The adsorption experiments were performed in a fixed-bed reactor that was placed in a thermostat water bath to control the temperature of experiments. The prepared desulfurization adsorbents with appropriate volume were put in a fixed-bed reactor. The model diesel fuel was poured into and flowed down through the fixed-bed reactor in which the DBT in fuel was adsorbed by the adsorbents adequately. The treated model diesel fuel was collected in a bulk tank followed by measuring its DBT content and calculating the desulfurization rate.

The adsorption equilibrium experiments were performed through the following procedures. Firstly, 0.5 g of C-PR, Zn–C, Ni–C, and Cu–C were put in volumetric flasks, and then 100 mL of solutions with different DBT concentrations were added respectively before sealing the flasks. The adsorption equilibrium was reached after oscillating in a thermostat water bath at 30 °C for 24 h. Trace amount of DBT solutions with different concentrations (100, 200, 300, 400, 500, 600, 700, and 800 mg L^{-1}) were put into a microcoulometer (WK-2D) to determine their sulfur contents through vaporization at 700 °C, combustion at 820 °C, and stabilization at 600 °C. Then, the standard curve of sulfur content versus DBT concentration could be drawn. From the standard curve, the DBT concentrations after adsorption were obtained according to their sulfur contents determined by microcoulometer. The absorption capacities of adsorbents at the adsorption equilibrium were calculated to draw the adsorption isotherm. Finally, the Freundlich and Langmuir equations were used to adsorption isotherm fitting.

The removal rate of DBT (*E*) is calculated by Eq. (1),

$$E(\%) = \frac{(c_0 - c_t)}{c_0} \times 100\% \quad (1)$$

where c_0 and c_t are the DBT concentrations before adsorption and at adsorption equilibrium, respectively.

The Freundlich and Langmuir equations are shown as Eqs. (2) and (3), respectively,

$$q_e = K_f (c_e)^{1/n} \quad (2)$$

$$\frac{c_e}{q_e} = \frac{1}{q_{max} \times K_L} + \frac{c_e}{q_{max}} \quad (3)$$

where q_e is the absorption capacity of the adsorbent at the adsorption equilibrium (mg g^{-1}), c_e is the DBT concentration at the adsorption equilibrium (mg L^{-1}), q_{max} is the maximum adsorption capacity of the adsorbent in theory (mg g^{-1}), $q_{max} \times K_L$ is the relative affinity of the adsorbate on the surface of the adsorbent, K_L is the Langmuir constant (mg^{-1}), and $1/n$ and K_f are the Freundlich constants.

Adsorption kinetics

C-PR, Zn–C, Ni–C, and Cu–C at 0.5 g were respectively added to 100 mL of the DBT solutions (300 mg L^{-1}). The mixtures were placed in sealed flasks and oscillated in a thermostat water bath at 30 °C. The supernatant was taken every certain time to measure the absorption capacities (q_t) of the adsorbents within a certain time (t). Finally, the q_t values were used as ordinate and the t values as abscissa to draw the kinetic curves of DBT adsorption on C-PR, Zn–C, Ni–C, and Cu–C.

Results and discussion

Structural properties of synthesized adsorbents

The specific surface area, total pore volume, and average pore diameter of C-PR and Zn–C are listed in Table 1. It can be found that the specific surface area and total pore volume of C-PR respectively decreases from 1182.1 to 809.7 m^2 g^{-1} and 0.152 to 0.074 mL g^{-1} after loading of Zn, which may be due to the adsorption and aggregation of metals on the external surface of activated carbon (Gao et al. 2011). However, Zn–C still possesses well-developed pore structure with average pore diameter of 0.735 nm, which meet the standard of microporous structure and is larger than the diameter of dibenzothiophene molecule (about 0.65 nm), indicating that dibenzothiophene can be adsorbed effectively by the synthesized adsorbent.

Table 1 Physicochemical characteristics of C-PR and Zn–C

Adsorbent	S_{BET}[a] (m^2 g^{-1})	P_d[b] (nm)	P_v[c] (mL g^{-1})
C-PR	1182.1	0.513	0.152
Zn–C	809.7	0.735	0.074

[a] Specific surface area

[b] Average pore diameter

[c] Total pore volume of the adsorbents

The morphologies of C-PR and Zn–C are shown in Fig. 1a–d. There is unobvious change for microstructures between C-PR (Fig. 1a, b) and Zn–C (Fig. 1c, d), and a number of aggregates can be found. Figure 1e, f display the TEM images of C-PR and Zn–C, respectively. PR-AC is homogeneous-sized spherical particles with average diameter of ca. 25 nm and has a rough surface covered by micropores whose volume governs the DBT adsorption amount (Ania and Bandosz 2005). The fuscous dots in Fig. 1f are ZnO particles, and the light matter is the PR-AC support whose particle diameter and morphology are not influenced by the loaded metal component. It can be noted that the active metal components also have some degree of agglomeration.

Desulfuration performance evaluation

Influence of adsorbent component

Figure 2 shows the DBT removal rates on three desulfurization adsorbents (Zn–C, Ni–C, and Cu–C) in dynamic adsorption. It is obvious that DBT removal rate on Zn–C is the highest while that on Cu–C is the lowest. The DBT removal rate increases firstly when low amount of metal species introduced, while the removal rate decreases to some extend when further raise the metal content. The reason is that appropriate enhancing the metal loading would make the metal components disperse highly and increase the adsorptive site quantity, while excess metal loading would cause metal phase aggregation and decrease the adsorptive site amount as well as plug the micropores, which play an important role in DBT adsorption. The highest DBT removal rate on Zn–C (89.14 %) is reached when Zn^{2+} loading is 0.2 mol L^{-1}. Compared with the desulfuration performance of pure PR-AC (34.4–45.6 %) (Fig. S1), the desulfuration performance of Zn–C, Ni–C, and Cu–C improves greatly (45–89 %), suggesting that these metal impregnation can enhance the interaction between DBT molecules and PR-AC surface. The loading of Zn^{2+}, Ni^{2+}, or Cu^{2+} changes the acid-base property of PR-AC support, which is closely related to the adsorption of DBT according to the hard-soft-acid-base (HSAB) principle (Pearson 1963). Xiao et al. (2008) has reported that loading of metal ions could enhance the adsorption of BT/DBT over activated carbon through weakening the local hard acids of adsorbent surface. Pan et al. investigated the adsorption performance of dichloromethane (DCM) over activated carbons (ACs) modified by metal ions and indicated that doping of metal ions could change the surface local acid hardness of ACs and hence affect the adsorption of DCM (Pan et al. 2013).

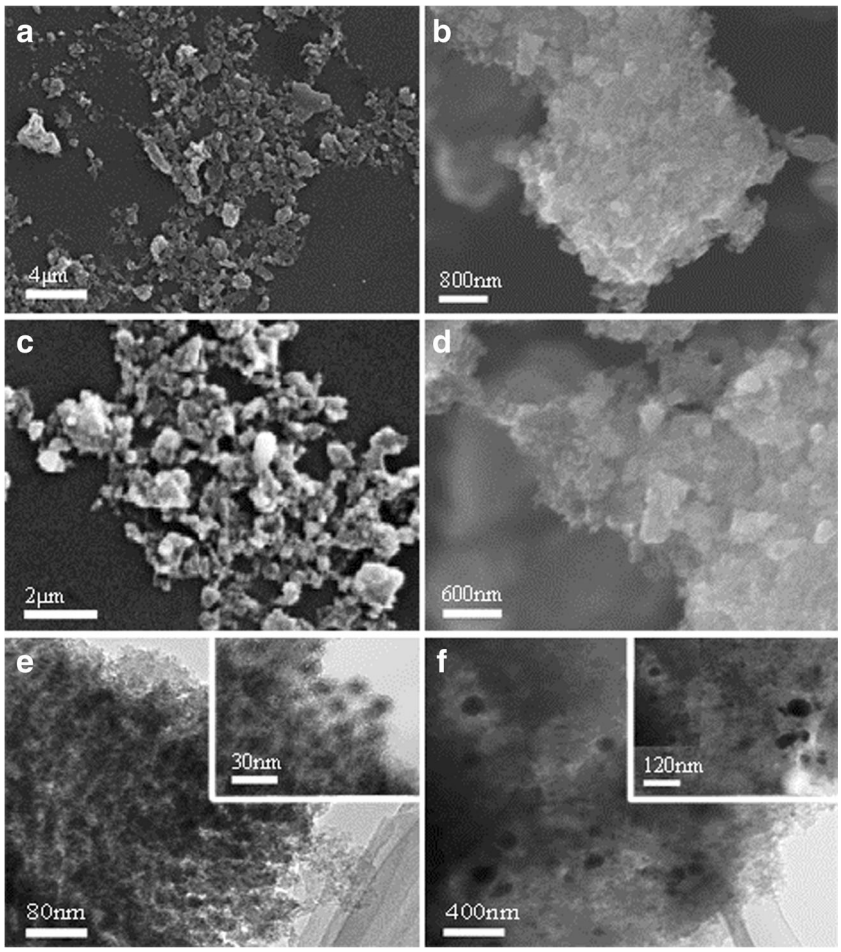

Fig. 1 SEM and TEM images of samples: **a**, **b** SEM images of C-PR, **c**, **d** SEM images of Zn–C, **e** TEM images of C-PR, and **f** TEM images of Zn–C

Influence of DBT concentration

The organic sulfur compound concentration of actual diesel fuel is usually different; the effect of DBT initial concentration on DBT removal efficiency over Zn–C, Ni–C, and Cu–C was investigated, as exhibited in Fig. 3. When the DBT concentration of the model diesel fuel is 300 mg L^{-1}, DBT could be removed efficiently, and the removal rates on Zn–C, Ni–C, and Cu–C reach 92.68, 86.47, and 68.13 %, respectively. However, the removal rates decrease sequentially with increasing the DBT concentration (especially for DBT concentration higher than 500 mg L^{-1}), implying that the adsorbents has been saturated by DBT, which is in agreement with previous work (Kumar and Srivastava 2012). This phenomenon can be explained by that the micropores and vacant adsorptive sites on the surface of adsorbents decrease due to the increasing of DBT concentration, resulting in the competition among DBT molecules. Besides, Xiao et al. (2012) has reported that other polyaromatics, O-containing diesel additives, nitrogen compounds, and moisture in real diesel fuels also show a negative effect on organic sulfur compound adsorption, so more work need be done to increase the selectivity and adsorption capacity of adsorbents.

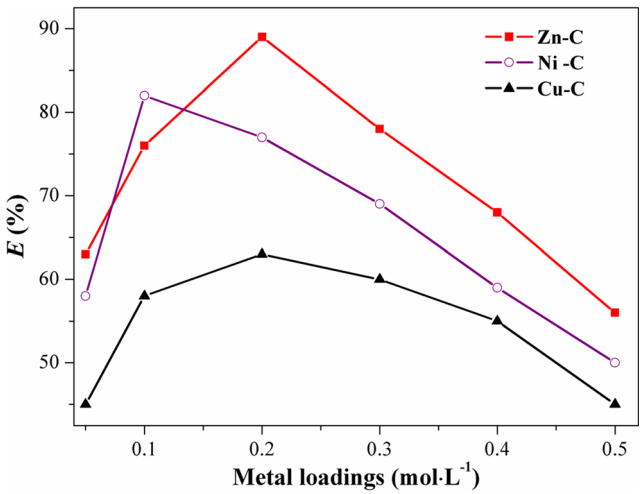

Fig. 2 Influence of adsorbent component on desulfurization rate (DBT, 500 mg L^{-1}; LHSV, 8.0 h^{-1}; adsorption time, 1 h; adsorption temperature, 30 °C)

Influence of liquid hourly space velocity

Liquid hourly space velocity (LHSV) is a significant factor that can change the retention time in adsorption system.

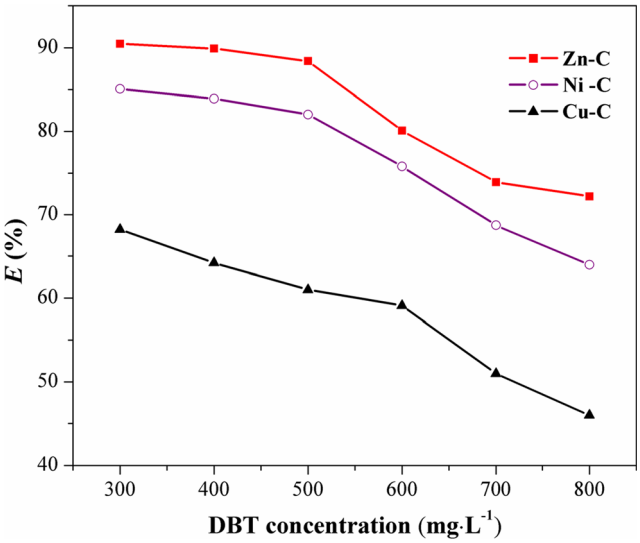

Fig. 3 Influence of DBT concentration on desulfurization rate (metal loading, 0.2 mol L^{-1}; LHSV, 8.0 h^{-1}; adsorption time, 1 h; adsorption temperature, 30 °C)

Figure 4 displays the DBT removal rates on Zn–C, Ni–C, and Cu–C with LHSV varied from 4 to 12 h^{-1}. It is found that when the LHSV is lower than 8 h^{-1}, the DBT removal rates of Zn–C, Ni–C, and Cu–C can respectively reach up to 89.14, 82.35, and 62.57 %, and DBT removal rates enhance with the LHSV increasing from 4 to 8 h^{-1}. The reason is that low LHSV can increase the mass transfer resistance and reduce the diffusion rate of DBT, making the contact between DBT molecules and adsorbents difficult. When the LHSV is higher than 8 h^{-1}, the DBT removal rates decrease as high LHSV reduces the retention time of model diesel fuel, which make DBT contact with the micropores and vacant adsorptive sites inadequately (Kong et al. 2013).

Influence of adsorption time

Adsorption time is also an important parameter that can directly affect the cost of desulphurization process and dosage of adsorbents. Figure 5 shows the influence of adsorption time varying from 0.25 to 2 h on DBT removal efficiency. As the adsorption time extended, the DBT removal rates of Zn–C, Ni–C, and Cu–C increase until the adsorption time is about 1.5 h, indicating that the adsorption equilibration is reached. Before achieving the adsorption equilibration, DBT contacts with the adsorbent more completely when prolong the adsorption time, and hence increases the DBT removal rate. The DBT removal rates of Zn–C, Ni–C, and Cu–C are 91.24, 87.45, and 73.38 %, respectively, when the adsorption time is 1.5 h. In the initial period, there were abundant vacant micropores and adsorptive sites on the surface of adsorbents so the majority of DBT was adsorbed within 1 h. Later, the adsorption curves became smooth, which may be due to that much larger resistance must be overcame when DBT diffused to deeper and interior micropores (Nejada et al. 2013; Xu et al. 2011).

Influence of adsorption temperature

The effect of adsorption temperature on the adsorption capacity of Zn–C, Ni–C, and Cu–C is shown in Fig. 6. Desulphurization rates of Zn–C, Ni–C, and Cu–C increased with the increasing of temperature, and the desulphurization rates respectively reach the maximum values of 94.17, 90.02, and 77.93 % at 50, 40, and 50 °C, while decrease thereafter. Although adsorption is generally an exothermic process, the adsorption of DBT over adsorbents appears to be controlled by DBT diffusion, which is an endothermic process at low

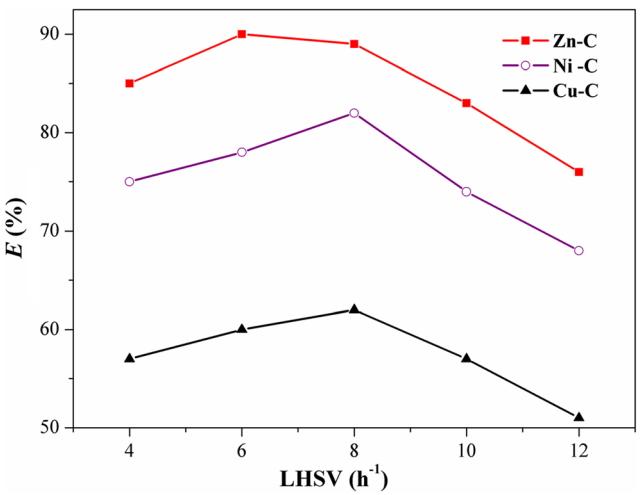

Fig. 4 Influence of liquid hourly space velocity on desulfurization rate (metal loading, 0.2 mol L^{-1}; DBT, 500 mg L^{-1}; adsorption time, 1 h; adsorption temperature, 30 °C)

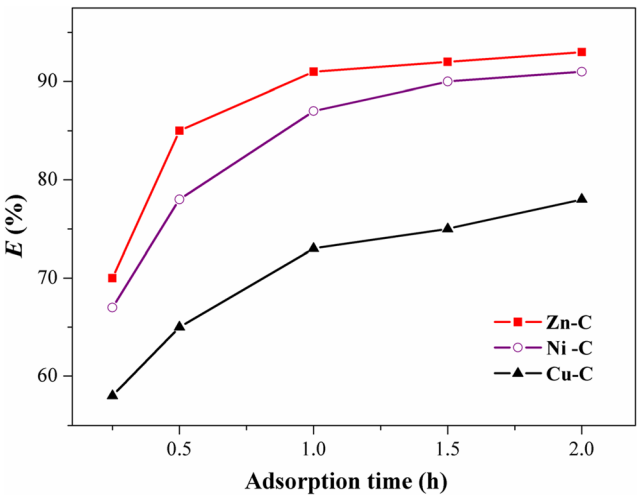

Fig. 5 Influence of adsorption time on desulfurization rate (metal loading, 0.2 mol L^{-1}; DBT, 500 mg L^{-1}; LHSV, 8.0 h^{-1}; adsorption temperature, 30 °C)

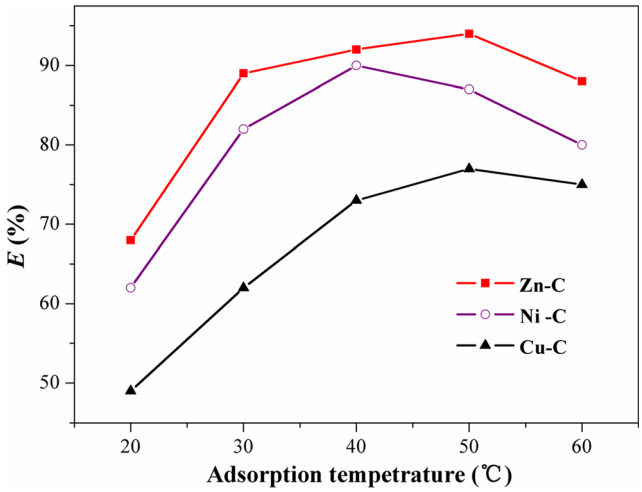

Fig. 6 Influence of adsorption temperature on desulfurization rate (metal loading, 0.2 mol L^{-1}; DBT, 500 mg L^{-1}; LHSV, 8.0 h^{-1}; adsorption time, 1 h)

temperature (Kumar and Srivastava 2012). Therefore, when the temperature is lower than 40 or 50 °C, the increasing of temperature can improve DBT diffusion rate and enhance the contact of DBT and the adsorbents. However, with the continuous increases of temperature and DBT diffusion rate, heat which was more than that assimilated in DBT diffusion released after bond formation between DBT and the adsorbents (Al-Degs et al. 2008; Mattson and Mark 1971). Thus, the adsorption equilibrium can be disturbed by further increasing the temperature, and DBT will be desorbed from the adsorbents.

Adsorption condition optimization

Above results reveal that appropriate metal loading, lower DBT concentration, appropriate LHSV, longer adsorption time, and appropriate adsorption temperature contribute to high removal rate of DBT over absorbent. According to the level factors in Table 2, an L_{16} orthogonal test was carried out to optimize the parameters from a limited number of experimental data. The experiment process can be described mathematically and obtain the highest DBT removal rate. Zn–C was used in the test due to its much better performance than that of the other adsorbents in previous studies. Results of the orthogonal test are shown in Table 3. It can be seen that the most influential factor is LHSV, followed by Zn^{2+} loading, adsorption temperature, adsorption time, and DBT concentration, and there is not much difference among the effect of these variables on DBT removal rate. Optimal adsorption conditions are adsorption temperature of 50 °C, DBT concentration of 300 mg L^{-1}, Zn^{2+} loading of 0.2 mol L^{-1}, LHSV of 8 h^{-1}, and adsorption time of 1 h, under which the highest desulphurization rate could achieve 92.36 %. The efficiency was excellent compared with the performance of other adsorbents reported in the literature (Table 4).

Table 2 Orthogonal factor level table

Factors	Zn^{2+} loading (mol L^{-1})	DBT concentration (mg L^{-1})	LHSV (h^{-1})	Adsorption temperature (°C)	Adsorption time (h)
1	0.05	300	4	20	0.5
2	0.1	400	6	30	1
3	0.2	500	8	40	1.5
4	0.3	600	10	50	2

Desulfuration mechanism

Adsorption product

The model diesel fuel used in this study was *n*-octane solution of DBT. GC-MS was used to identify the constituent of the model diesel fuel and analysis the original and treated model diesel fuel, and only *n*-octane and DBT can be detected in the treated model diesel fuel (not shown). In addition, just a trace amount of DBT can be detected in the treated model diesel fuel, while the amount of *n*-octane in the treated model diesel fuel is almost unchanged compared with that of the original model diesel fuel, indicating that DBT could be removed effectively by the adsorbent without reducing the property of the model diesel fuel.

Adsorbent surface property

The FT-IR spectra of C-PR and Zn–C before and after adsorption are shown in Fig. 7. It is obvious that some characteristic peaks appear in the FT-IR spectra of C-PR and Zn–C after adsorption, implying large amounts of DBT exist in the adsorbents. As shown in FT-IR spectra of C-PR before and after adsorption (Fig. S2), multiple peaks appeared at 2917 cm^{-1} are stretching vibration absorption of C–H bonds in aromatic ring. The bands in 1700 to 1500 cm^{-1} can be identified as the adsorption of thiophenes derivative which increases due to the influence of substituent groups with electronic withdrawing ability. Two small weak peaks in 740 to 700 cm^{-1} are the characteristic peaks of DBT. Therefore, DBT could be adsorbed by C-PR and Zn–C effectively. It can also be inferred from the FT-IR results that the adsorption of DBT on Zn–C is stronger than that on C-PR because the loading of Zn^{2+} improves the heterogeneity of PR-AC surface, which promotes the adsorption process (Fig. S2).

Adsorption model

The Langmiur and Freundlich equations which were reported to be suitable to explain the adsorption behavior of DBT on activated carbon (Ania and Bandosz 2006). Fitting results of

Table 3 Multi-factor orthogonal test results

Experiment no.	Zn^{2+} loading (mol L^{-1})	DBT concentration (mg L^{-1})	LHSV (h^{-1})	Adsorption temperature (°C)	Adsorption time (h)	*E* (%)
1	0.05	300	4	20	0.5	45.23
2	0.05	400	6	30	1	63.14
3	0.05	500	8	40	1.5	88.37
4	0.05	600	10	50	2	76.44
5	0.1	300	6	40	2	55.12
6	0.1	400	4	50	1.5	65.31
7	0.1	500	10	20	1	67.25
8	0.1	600	8	30	0.5	78.83
9	0.2	300	8	50	1	92.36
10	0.2	400	10	40	0.5	85.46
11	0.2	500	4	30	2	67.49
12	0.2	600	6	20	1.5	71.38
13	0.3	300	10	30	1.5	83.56
14	0.3	400	8	20	2	72.49
15	0.3	500	6	50	0.5	65.32
16	0.3	600	4	40	1	76.81
Average 1	68.295	69.067	63.710	64.087	67.460	
Average 2	65.377	71.600	63.740	72.005	74.890	
Average 3	79.172	72.108	81.763	76.440	77.155	
Average 4	74.545	74.615	18.177	74.858	67.885	
Range	13.795	5.548	18.053	12.353	9.695	

the Langmiur model for DBT adsorption over C-PR, Zn–C, Ni–C, and Cu–C samples are shown in Table 5 and Fig. 8. The correlation coefficients ($R^2 > 0.98603$) indicate that the experimental data are fitted well with the Langmiur model. Ni–C, Cu–C, and especially Zn–C (R^2 = 0.99713) have better goodness of fit compared with that of C-PR, implying that the impregnation of metal cations can enhance the adsorption capacity of PR-AC due to the improvement of surface heterogeneity, which is in line with previous work (Xiao et al. 2008, 2010; Xiong et al. 2012; Moosavi et al. 2012). The increase of

Table 4 Comparison of performance of various commercial adsorbents for sulfur removal

Adsorbent	Adsorbate	Model oil	c_0 (mg S/L)	Adsorption temperature (°C)	q_e (mg g^{-1})	*E* (%)	Reference
Zn–C	DBT	*n*-octane	52	50	18.24	92.36	This work
Activated alumina	DBT	*n*-hexane	500	30	–	~58	Srivastav and Srivastava (2009)
Nb(5) ZSM-5	Thiophene	*iso*-octane *n*-octane	808.50	80	46.3	73.6	Cavalcanti et al. (2013)
Bamboo charcoal	DBT	*n*-octane	–	–	–	67.9	Zhao et al. (2008)
ACFH-Cu^{+}	DBT	*n*-hexane	–	Room temperature	–	~40	Moosavi et al. (2012)
AC	Total sulfur	Diesel	–	30–70	0.1742	67.4	Muzic et al. (2010)
Ag^{I}/AC	DBT	*n*-octane	320	30	~23.36	–	Xiao et al. (2008)
CAC	DBT	*n*-octane	100	30	–	53	Kumar and Srivastava (2012)
Ce/AC	DBT	Petroleum ether	–	30	~13	–	Xiong et al. (2012)
PS-Cu	DBT	Hexane	–	30	~58	67	Ania and Bandosz (2006)
Cu(I)Y	DBT	–	–	–	25.27	–	Wang et al. (2011)
$PdCl_2$/AC830	DBT	n-octane	–	20	5.44	–	Vilarrasa-Garciía et al. (2010)

ACFH hydrogen-treated activated carbon fiber, *CAC* commercial activated carbon, *PS* polystyrene-based activated carbon

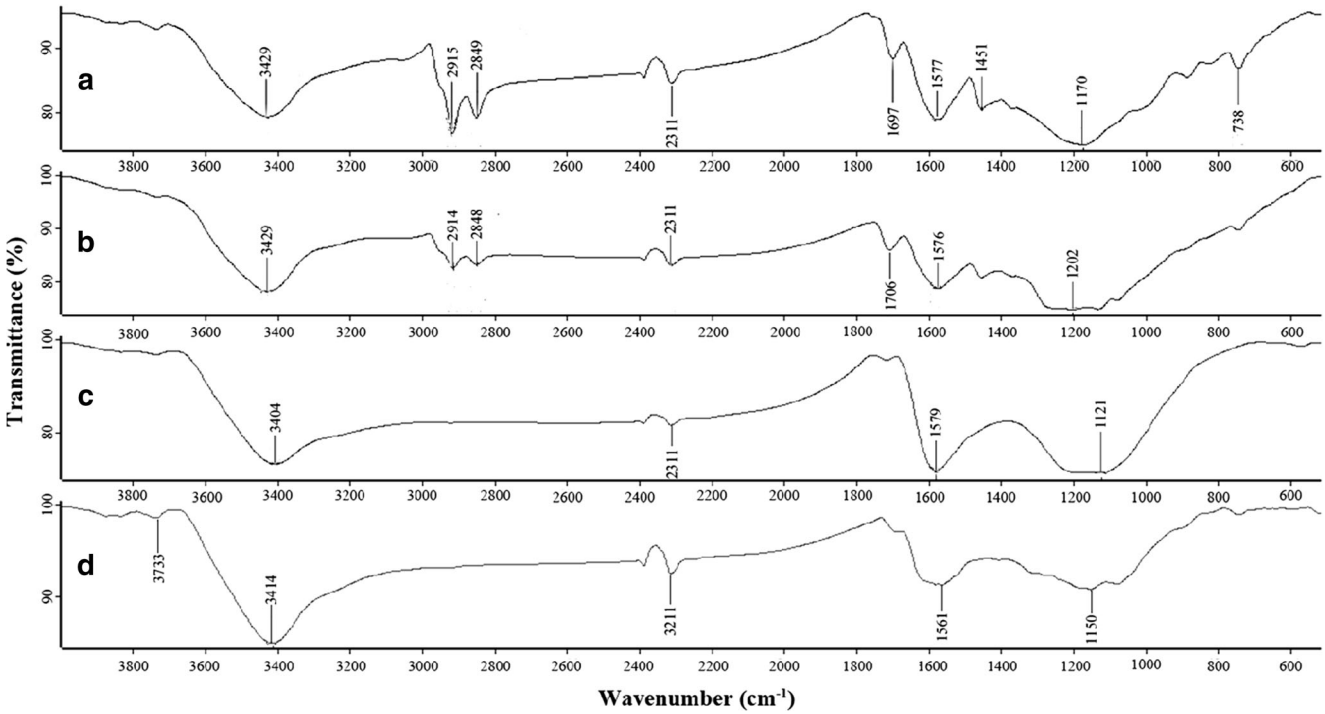

Fig. 7 FT-IR spectra of C-PR and Zn–C: **a** Zn–C after adsorption, **b** C-PR after adsorption, **c** Zn–C before adsorption, and **d** C-PR before adsorption

q_{max} values of Zn–C, Ni–C, and Cu–C indicates the increase of the maximum theoretical adsorption capacity due to the change of local hardness of the activated carbon surface caused by the metal incorporation (Yu et al. 2007).

In order to explain the effect of local hardness of activated carbon surfaces on the adsorption of DBT, the HSAB principle was locally applied, that is, "hard regions of a system prefer to interact with hard reagents whereas soft regions prefer soft species" (Pearson 1963). According to density functional theory (DFT) used by Parr and Pearson (1983) and Pearson's classification, DBT is considered a soft base and the ions Zn^{2+}, Ni^{2+}, and Cu^{2+} are borderline acids. When the ions of Zn^{2+}, Ni^{2+}, and Cu^{2+} are loaded on the surface of activated carbon, the local hard acid of the surface is weaken, which enhances the adsorption of DBT. Furthermore, the π-complexation on the surface of Zn–C and Ni–C also plays an important role in DBT adsorption, resulting in their stronger adsorption than that of Cu–C as cupper ion is diatomic and is not capable of π-complexation (Hernández-Maldonado and Yang 2003). Moosavi et al. (2012) studied the effect of copper or nickel ions with different valences on the adsorption of TC and reported that the adsorption mechanism can be explained by both HSAB principle and π-complexation. It can be deduced that the adsorption of DBT over Zn–C, Ni–C, or Cu–C is influenced by HSAB principle and π-complexation simultaneously, and the π-complexation is the main factor enhancing the adsorption capacity of DBT.

The adsorption of C-PR, Zn–C, Ni–C, and Cu–C was further investigated by fitting the experimental data with the Freundlich model, and the goodness of fit is inferior to that of the Langmiur odel (Table S2; Fig. S3). The coefficient, $1/n$ is less than 1.0 and larger than 0, indicating the physical adsorption (Muzic et al.

Table 5 Langmuir isotherm parameters and correlation coefficients for DBT adsorption

Adsorbent	q_{max} (mg g^{-1})	K_L (1 mg^{-1})	$q_{max} \times K_L$	R^2
C-PR	57.937	0.00563	0.37832	0.98603
Zn–C	176.64	0.00653	0.99449	0.99713
Ni–C	134.23	0.00363	0.48691	0.99067
Cu–C	96.993	0.00477	0.46278	0.98779

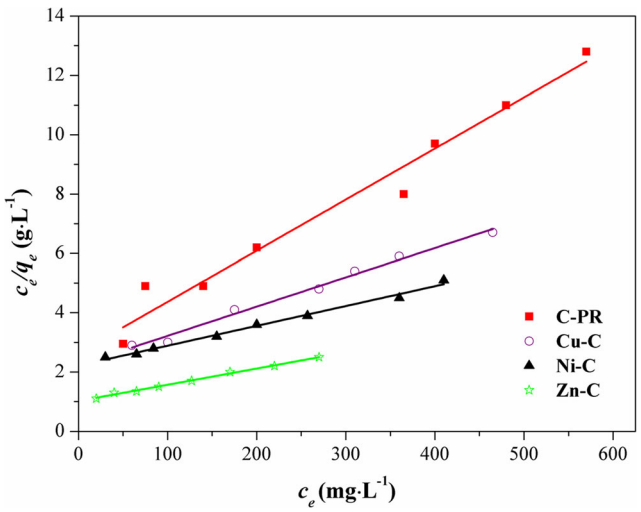

Fig. 8 Fitting results of the Langmuir model

2008), so the adsorption capacity of DBT decreases with the decrease of the vacant adsorptive sites.

Adsorption kinetics

Various kinetic models including the pseudo-first-order model, pseudo-second-order model, and intraparticle diffusion model were used to explore the adsorption process for C-PR, Zn–C, Ni–C, and Cu–C and determine the controlling step of adsorption. In the pseudo-first-order model and pseudo-second-order model, adsorption of DBT molecules from *n*-octane to the *s* adsorbent is considered a reversible process with equilibrium being established between the solution and the solid phase (Abu Safieh et al. 2015).

The pseudo-first-order model is expressed as Eq. (4):

$$\lg(q_e - q_t) = \lg q_e - \frac{k_1}{2.303} t \quad (4)$$

where q_e is the absorption capacity of the adsorbent at the adsorption equilibrium (mg g^{-1}), q_t is the absorption capacity of the adsorbent at the time, t (mg g^{-1}), t is adsorption time (min), and k_1 is the rate constant of the first-order adsorption (min^{-1}). The pseudo-first-order model is the most widely used in adsorption of a solute from a liquid solution, in which the regression of $\lg(q_e - q_t)$ versus t is a linear relationship (Ho et al. 2000).

The pseudo-second-order model is expressed as Eq. (5):

$$\frac{t}{q_t} = \frac{1}{k_2 q_e^2} + \frac{t}{q_e} \quad (5)$$

where k_2 is the rate constant of the second-order adsorption (g mg^{-1} min^{-1}). In the pseudo-second-order model, no other parameter need to be known beforehand but only q_e and k_2 that can be obtained from slope and intercept. The application is determined by judging if the plot of t/q_t against t is a linear relationship (Ho et al. 2000).

The intraparticle diffusion model is expressed as Eq. (6):

$$q_t = k_d t^{\frac{1}{2}} \quad (6)$$

where k_d is the rate constant of the intraparticle diffusion(g mg^{-1} $min^{-1)}$.

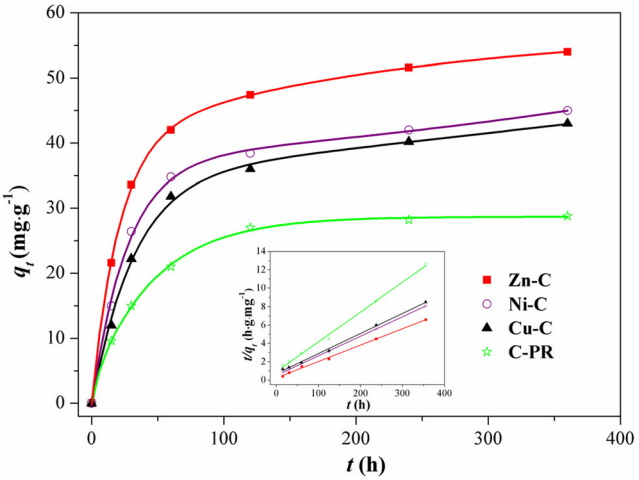

Fig. 9 DBT adsorption rate on various desulfurization adsorbents

The results of the kinetic study are presented in Table 6 and Fig. 9. The correlation coefficients (R^2) of the pseudo-second-order model are higher than 0.99312, while those of the pseudo-first-order model and intraparticle diffusion model are less than 0.96919 and 0.93525, respectively, suggesting that the pseudo-second-order model is more appropriate to describe the adsorption kinetics of DBT over C-PR, Zn–C, Ni–C, and Cu–C. In addition, the regression of t/q_t versus t is a linear relationship, which also indicates the good applicability of the pseudo-second-order model on the adsorption process, in accordance with the previous work (Muzic et al. 2008; Zhao et al. 2008; Abu Safieh et al. 2015). As shown in Table 6, although the rate constants of the adsorption are reduced because of the loading of metal, the adsorption kinetics properties are unchanged. Moreover, the adsorption performance of Zn–C, Ni–C, and Cu–C shown in Fig. 9 are better than that of C-PR.

Like adsorption behaviors of DBT over other porous absorbents (Jiang and Ng 2010; Srivastav and Srivastava 2009), the adsorption capacity of DBT over C-PR, Zn–C, Ni–C, and Cu–C increases rapidly with adsorption time at first, and then increases slightly and finally tends to a constant with time extension, as shown in Fig. 9. The adsorption initially occurs on the surface of the

Table 6 Adsorption rate constants and correlation coefficients of various models

Adsorbent	c_0 (mg L^{-1})	Pseudo-first-order model		Pseudo-second-order model		Intraparticle diffusion model	
		K_1	R^2	K_2	R^2	K_d	R^2
C-PR	300	21.71	0.96919	0.001062	0.99312	3.5598	0.90739
Zn–C	300	12.15	0.92085	0.000124	0.99879	2.9066	0.91643
Ni–C	300	17.36	0.94119	0.000255	0.99733	2.7248	0.93525
Cu–C	300	18.23	0.95938	0.000349	0.99621	1.8927	0.92599

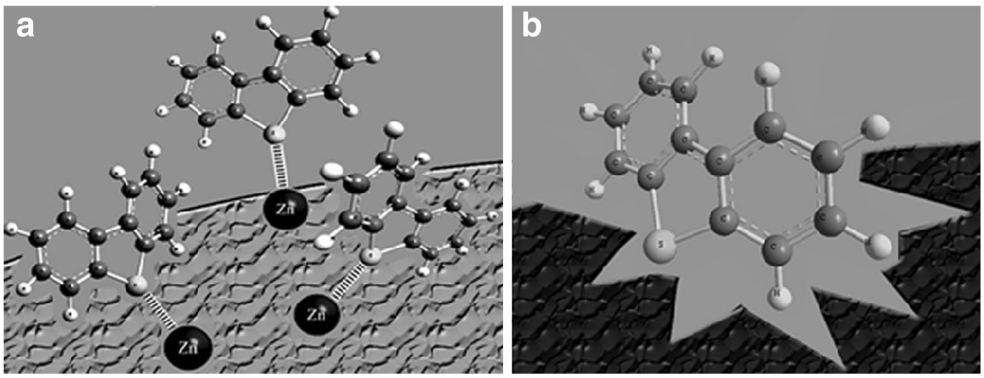

Fig. 10 Proposed adsorption process of DBT on C-PR and Zn–C: **a** C-PR and **b** Zn–C

adsorbents, and DBT diffuses into the micropores on the surface in a short time resulting on the decrease of DBT concentration. Along with the diffusion, resistance increases resulting the decrease of diffusion rate. In the diffusion process, the adsorption rate is controlled by the diffusion rate, so the adsorption rate decreased. In the adsorption anaphase, the adsorption mainly occurs on the internal surface of the adsorbents and reaches the dynamic equilibrium with the smaller and smaller concentration driving force (Faust and Aly 1983).

Proposed adsorption mechanism

The adsorption mechanisms of DBT over C-PR and Zn–C are given, as shown in Fig. 10. As for the adsorption of DBT over C-PR (Fig. 10b), DBT is adsorbed into the micropores on the surface of C-PR by the van der Waals force, which depends on the good matchability between the sizes of DBT molecules and micropores, so appropriate pore structure and diameter are important for DBT adsorption over pure activated carbon. However, the DBT adsorption over Zn–C is not only related to the micropores on the surface of the adsorbents but also to the active absorption sites formed by Zn. According to previous work (Song and Ma 2003; Velu et al. 2003), eight known different coordination geometries of thiophen in organometallic complexes are classified as direct S–M bond, π-complexation, and geometries involving both direct S–M bonds and π-complexations. There are two pairs of electrons on the S atom of DBT. One pair of them is in the plane of the molecule ring and can form direct S–M bond with metal or metal ions when DBT acts as an n-type donor. Another pair of electrons is in the six-electron π system and can form π-complexation with metal or metal ions when DBT acts as a π-type donor. As shown in Fig. 10a, there is a π-complexation between S atom of DBT and Zn^{2+}. The bond energy of π-complexation is much stronger than that of van der Waals interactions, so the selective adsorption of DBT over the PR-AC loaded with active metal component is stronger than the physical adsorption on pure PR-AC although the specific surface area of Zn–C is reduced. This also indicates that the adsorption of DBT on the prepared adsorbents is dominanted by the π-complexation.

Conclusions

PR-AC-loaded Zn, Ni, or Cu with well-developed pore structure and high specific surface area were prepared by impregnation method to remove DBT in the model diesel fuel by adsorption. The following conclusions are obtained:

(1) PR-AC-loaded metal adsorbents can enhance the adsorption capacity towards DBT greatly. The loading of metal cations decreases the specific surface area and total pore volume of PR-AC support, but increases the average pore diameter, which contributes to the enhancement in adsorption capacity. Zn–C presents the highest adsorption capacity towards DBT followed by Ni–C and Cu–C.

(2) High initial DBT concentration is negative to DBT adsorption. DBT adsorption can be improved by increasing LHSV, adsorption time and temperature properly. DBT removal rate could reach up to 92.36 % with adsorption temperature of 50 °C, DBT concentration of 300 mg L^{-1}, Zn^{2+} loading of 0.2 mol L^{-1}, LHSV of 8 h^{-1}, and adsorption time of 1 h.

(3) The Langmiur model fits the adsorption data better than the Freundlich model. Adsorption kinetic can be illustrated by the pseudo-second-order model. The adsorption of DBT over PR-AC-loaded metal adsorbents is selective adsorption governed by not only micropore adsorption but also the specific interactions between DBT molecules and metal ions involving acid-base interactions and π-complexation. The π-complexation existing between S atom in DBT and metal ions is the main factor enhancing the DBT adsorption over PR-AC-loaded metal adsorbents. The desulfurization adsorbents obtained via widely applicable PR-AC and economical divalent metal (Zn, Ni, or Cu) are promising to be applied and commercialized in deep desulfurization of diesel fuel.

Acknowledgments Financial supports of the National Key Research and Development Program (2016YFC0204201), the National Natural Science Foundation of China (21677114, 21477095), the Industrial Research Project of Science and Technology of Shaanxi Province (2016GY-243), the Postdoctoral Science Foundation of China (2014M550498), and the Natural Science Basic Research Plan in Shaanxi Province of China (2015JM2047). The authors are also grateful to the reviewers and the editor for their helpful comments.

References

Abu Safieh KA, Al-Degsa YS, Sunjuka MS, Saleha AI, Al-Ghoutib MA (2015) Selective removal of dibenzothiophene from commercial diesel using manganese dioxide-modified activated carbon: a kinetic study. Environ Technol 36:98–105

Al-Degs YS, El-Barghouthi MI, El-Sheikh AH, Walker GM (2008) Effect of solution pH, ionic strength, and temperature on adsorption behavior of reactive dyes on activated carbon. Dyes Pigments 77: 16–23

Ania CO, Bandosz TJ (2005) Importance of structural and chemical heterogeneity of activated carbon surfaces for adsorption of dibenzothiophene. Langmuir 21:7752–7759

Ania CO, Bandosz TJ (2006) Metal-loaded polystyrene-based activated carbons as dibenzothiophene removal media via reactive adsorption. Carbon 44:2404–2412

Bhatia S, Sharma DK (2012) Thermophilic desulfurization of dibenzothiophene and different petroleum oils by Klebsiella sp. 13 T. Environ Sci Pollut Res 19:3491–3497

Cavalcanti RM, Barros ICL, Dias JA, Dias SCL (2013) Characterization of ZSM-5 modified with niobium pentoxide: the study of thiophene adsorption. Braz Chem Soc 24:40–50

Cavalcantia RM, Pessoa Júniora WAG, Bragab VS, Barrosa ICL (2015) Adsorption of sulfur compound utilizing rice husk ash modifiedwith niobium. Appl Surf Sci 355:171–182

Cychosz KA, Wong-Foy AG, Matzger AJ (2009) Enabling cleaner fuels: desulfurization by adsorption to microporous coordination polymers. J Am Chem Soc 31:14538–14543

Dharaskar SA, Wasewar KL, Varma MN, Shende DZ (2015) Synthesis, characterization, and application of 1-butyl-3-methylimidazolium thiocyanate for extractive desulfurization of liquid fuel. Environ Sci Pollut Res. doi:10.1007/s11356-015-4945-1

Dhawan R, Bhasin KK, Goyal M (2015) Isotherms, kinetics and thermodynamics for adsorption of pyridine vapors on modified activated carbons. Adsorption 1:37–52

Fallah RN, Azizian S, Dwivedi AD, Sillanpaa M (2014) Adsorptive desulfurization using different passivated carbon nanoparticles by PEG-200. Fuel Proc. Technol. 130:214–223

Faust DS, Aly MO (1983) Adsorption Processes for Water Treatment. Butterworths, Boston

Gao X, Liu S, Zhang Y, Luo Z, Cen K (2011) Physicochemical properties of metal-doped activated carbons and relationship with their performance in the removal of SO_2 and NO. J Hazard Mater 188:58–66

Hernández-Maldonado AJ, Yang RT (2003) Desulfurization of liquid fuels by adsorption via π- complexation with Cu(I)-Y and Ag-Y zeolites. Ind Eng Chem Res 42:123–129

Hernández-Maldonado AJ, Yang RT (2004a) Desulfurization of transportation fuels by adsorption. Catal Rev Sci Eng 46:111–150

Hernández-Maldonado AJ, Yang RT (2004b) Desulfurization of diesel fuels by adsorption via π-complexation with vapor-phase exchanged Cu(I)-Y zeolites. J Am Chem Soc 126:992–993

Hernández-Maldonado AJ, Yang RT (2004c) Desulfurization of diesel fuels via π-Complexation with nickel(II)-exchanged X- and Y-zeolites. Ind Eng Chem Res 43:1081–1089

Hernández-Maldonado AJ, Yang RT (2004d) New sorbents for desulfurization of diesel fuels via π-complexation. AICHE J 50:791–801

Ho YS, Ng JC, McKay G (2000) Kinetics of pollutants sorption by biosorbents: review. Sep Purif Method:29189–29232

Irvine RL (1998) US Patent 5 730 860

Jiang J, Ng FTT (2010) Production of low sulfur diesel fuel via adsorption: an equilibrium and kinetic study on the adsorption of dibenzothiophene onto NaY zeolite. Adsorption 16:549–558

Khare GP, Engelbert DR, Cass BW (2000) US Patent 6 056 871

Kong A, Wei Y, Li Y (2013) Reactive adsorption desulfurization over a Ni/ZnO adsorbent prepared by homogeneous precipitatio. Front Chem Sci Eng 7:170–176

Kulkarni PS, Afonso CAM (2010) Deep desulfurization of diesel fuel using ionic liquids: current status and future challenges. Green Chem 12:1139–1149

Kumar DR, Srivastava VC (2012) Studies on adsorptive desulfurization by activated carbon. Clean Soil Air Water 40:545–550

Lei C, Markoulidis WP, Tennisonb S, Lekakou C (2013) Activated carbon N. Amini, F. From phenolic resin with controlled mesoporosity for an electric double-layer capacitor (EDLC). J Mater Chem A 1: 6037–6042

Mattson J, Mark H (1971) Activated carbon: surface chemistry and adsorption from solution. Marcel Dekker, New York

Moosavi ES, Dastgheib SA, Karimzadeh R (2012) Adsorption of thiophenic compounds from model diesel fuel using copper and nickel impregnated activated carbons. Energies 5:4233–4250

Muzic M, Sertic-Bionda K, Gomzi Z (2008) Kinetic and statistical studies of adsorptive desulfurization of diesel fuel on commercial activated carbons. Chem Eng Technol 31:355–364

Muzic M, Sertic-Bionda K, Gomzi Z, Podolski S, Telen S (2010) Study of diesel fuel desulfurization by adsorption. Chem Eng Res Des 88: 487–495

Nakagawa K, Mukai SR, Tamura K, Tamon H (2007) Mesoporous activated carbons from phenolic resins. Chem Eng Res Des 85:1331–1337

Nejada NF, Shamsa E, Aminia MK, Bennettb JC (2013) Synthesis of magnetic mesoporous carbon and its application for adsorption of dibenzothiophene. Fuel Process Technol 106:376–384

Pan H, Tian M, Zhang H, Zhang Y, Lin Q (2013) Adsorption and desorption performance of dichloromethane over activated carbons modified by metal ions. J Chem Eng Data 58:2449–2454

Parr RG, Pearson RG (1983) Absolute hardness: companion parameter to absolute electronegativity. J Am Chem Soc 105:7512–7516

Pearson RG (1963) Hard and soft acids and bases. J Am Chem Soc 85: 3533–3539

Reed LE, Bares JE, Dodwell GW, Gislason JJ, Morton RW, Sughrue EL, Johnson MJ, Malandra JL (2003) US Patent 6 656 877

Seredych M, Bandosz TJ (2010) Adsorption of dibenzothiophenes on activated carbons with copper and iron deposited on their surfaces. Fuel Proc Technol 91:693–701

Seredych M, Lison J, Jans U, Bandosz TJ (2009) Textural and chemical factors affecting adsorption capacity of activated carbon in highly efficient desulfurization of diesel fuel. Carbon 47:2491–2500

Singh A, Lal D (2008) Microporous activated carbon spheres prepared from resole-type crosslinked phenolic beads byphysical activation. Appl Polym Sci 110:3283–3291

Song C, Ma X (2003) New design approaches to ultra-clean diesel fuels by deep desulfurization and deep dearomatization. Appl Catal B Environ 41:207–238

Srivastav A, Srivastava VC (2009) Adsorptive desulfurization by activated alumina. J Hazard Mater 170:1133–1140

Srivastava VC (2012) An evaluation of desulfurization technologies for sulfur removal from liquid fuels. RSC Adv 2:759–783

Stanislaus A, Marafi A, Rana MS (2010) Recent advances in the science and technology of ultra low sulfur diesel (ULSD) production. Catal Today 153:1–68

Tennison SR (1998) Phenolic-resin-derived activated carbons. Appl Catal A: General 173:289–311

Thaligari SK, Srivastava VC, Prasad B (2016) Adsorptive desulfurization by zinc-impregnated activated carbon: characterization, kinetics, isotherms, and thermodynamic modeling. Clean Techn Environ Policy 18:1021–1030

Velu S, Ma X, Song C (2003) Selective adsorption for removing sulfur from jet fuel over zeolite-based adsorbents. Ind Eng Chem Res 42:5293–5304

Vilarrasa-Garciía E, Infantes-Molina A, Moreno-Tost R, Rodriíguez-Castelloín E, Jiménez-Loípez A, Cavalcante CL Jr et al (2010) Thiopheneadsorption on microporous activated carbons impregnated with $PdCl_2$. Energy Fuel 24:3436–3442

Wang Q, Liang X, Zhang R, Liu C, Liu X, Qiao W, Zhan L, Ling L (2009) Preparation of polystyrene-based activated carbon spheres and their adsorption of dibenzothiophene. New Carbon Mater 24:55–60

Wang L, Sun Z, Ding Y, Chen Y, Li Q, Xu M, Li H, Song L (2011) A theoretical study of thiophenic compounds adsorption on cation-exchanged Y zeolites. Appl Surf Sci 257:7539–7544

Xiao J, Bian G, Zhang W, Li Z (2010) Adsorption of dibenzothiophene on Ag/Cu/Fe-supported activated carbons prepared by ultrasonic-assisted impregnation. J Chem Eng Data 55:5818–5823

Xiao J, Li Z, Liu B, Xia Q, Yu M (2008) Adsorption of benzothiophene and dibenzothiophene on ion-impregnated activated carbons and ion-exchanged Y zeolites. Energy Fuel 22:3858–3863

Xiao J, Song C, Ma X, Li Z (2012) Effects of aromatics, diesel additives, nitrogen compounds, and moisture on adsorptive desulfurization of diesel fuel over activated carbon. Ind Eng Chem Res 51:3436–3443

Xiao J, Wang X, Fujii M, Yang Q, Song C (2013) A novel approach for ultra-deep adsorptive desulfurization of diesel fuel over TiO_2-CeO_2/MCM-48 under ambient conditions. AICHE J 59:1441–1445

Xiong L, Chen F, Yan X, Mei P (2012) The adsorption of dibenzothiophene using activated carbon loaded with cerium. J Porous Mater 19:713–719

Xu WZ, Zhou W, Bian LH, Huang WH, Wu XY (2011) Preparation of molecularly imprinted polymer by surface imprinting technique and its performance for adsorption of dibenzothiophene. J Sep Sci 34: 1746–1753

Yang RT, Hernández-Maldonado AJ, Yang FH (2003) Desulfurization of transportation fuels with zeolites under ambient conditions. Science 301:79–81

Yang J, Ling L, Liu L, Kang F, Huang Z, Wu H (2002) Preparation and properties of phenolic resin-based activated carbon spheres with controlled pore size distribution. Carbon 40:911–916

Yu F, Wang R (2013) Deep oxidative desulfurization of dibenzothiophene in simulated oil and real diesel using heteropolyanion-substituted hydrotalcite-like compounds as catalysts. Molecules 18:13691–13704

Yu M, Li Z, Xia Q, Xi H, Wang S (2007) Desorption activation energy of dibenzothiophene on the activated carbons modified by different metal salt solutions. Chem Eng J 132:233–239

Zhang S, Zhang Y, Huang S, Wang P, Tian H (2012) Mechanistic investigations on the adsorption of thiophene over Zn_3NiO_4 bimetallic oxide cluster. Appl Surf Sci 258:10148–10153

Zhao X, Lai S, Liu H, Gao L (2009) Preparation and characterization of activated carbon foam from phenolic resin. J Environ Sci 21:121–123

Zhao D, Zhang J, Duan E, Wang J (2008) Adsorption equilibrium and kinetics of dibenzothiophene from *n*-octane on bamboo charcoal. Appl Surf Sci 254:3242–3247